JOURNAL OF APPLIED ELECTROCHEMISTRY **26** (1996) 1185–1193

Interaction of aqueous silver ions with the surface of pyrite

L. M. MADDOX, G. M. BANCROFT, J. W. LORIMER

Department of Chemistry, The University of Western Ontario, London, Ontario, N6A 5B7, Canada

Received 26 October 1995; revised 26 February 1996

Electrochemical techniques (cyclic and linear sweep voltammetry) at rotating and stationary pyrite electrodes were used to study the interaction of pyrite with silver ions in nitrate supporting electrolyte, pH 3 and room temperature. At potentials just negative of the open circuit potential of pyrite, metallic silver was deposited by a nucleation-growth mechanism. Evidence for a surface ion exchange involving removal of Fe^{2+} from pyrite and replacement with silver ion was found (i) from an analysis of peak potentials for voltammograms taken after various immersion times and (ii) from the appearance of a peak at potentials negative to that for deposition of silver.

1. Introduction

Many leaching processes have been investigated for the recovery of copper from copper sulfide concentrates, such as those consisting mainly of chalcopyrite ($CuFeS_2$). A leaching system that has been studied extensively is aqueous acidic iron (III) sulfate [1]. In sulfuric acid solutions of iron (III) sulfate, chalcopyrite undergoes the following net reaction [1, 2]:

$$CuFeS_2(s) + 4Fe^{3+} \longrightarrow Cu^{2+} + 5Fe^{2+} + 2S(s) \tag{1}$$

The sulfur deposit was found to be a smooth and tenacious layer. The rate-limiting process in the dissolution of chalcopyrite was assumed to be transport of electrons through the elemental sulfur layer [1].

It is known that the addition of small amounts of silver ions to an acidic oxidation leach enhances the rate of reaction significantly. This information led to the development of a silver-catalysed acidic iron (III) sulfate leach. The role of silver ion as a catalyst for the enhanced dissolution of chalcopyrite as well as the regeneration of silver is proposed to be [1, 2]

$$CuFeS_2(s) + 4Ag^+ \longrightarrow 2Ag_2S(s) + Cu^{2+} + Fe^{2+} \tag{2}$$

$$2Fe^{3+} + Ag_2S(s) \longrightarrow 2Fe^{2+} + 2Ag^+ + S(s) \tag{3}$$

with Reaction 1 as the overall reaction. There are two possible explanations for enhancement of the reaction rate. One explanation is that a porous sulfur deposit forms instead of the tenacious deposit formed in the absence of the catalyst, leading to an increase in the limiting current due to electron transport across the sulfur layer.The other possibility [3] is that silver sulfide provides cathodic sites on the surface thereby increasing the rate of electron transfer across the sulfur layer compared to the uncatalysed reaction.

Pyrite (FeS_2) is a very common sulfide mineral and is found in a wide range of geological sites [4], and is one of the most common gold-bearing sulfide minerals [4, 5]. The leaching of precious metals from pyrite ores may pose the same problem of the formation of a tenacious layer of elemental sulfur which could inhibit the leaching rate. Hiskey *et al.* [4, 5] investigated the possibility of increasing the oxidation rate of pyrite by the addition of silver ions to an acidic iron (III) sulfate leach, as discussed above for chalcopyrite. The results suggested that elemental silver and elemental sulfur were the main products:

$$FeS_2(s) + 2Ag^+ \longrightarrow Fe^{2+} + 2S(s) + 2Ag(s) \tag{4}$$

It was also proposed that elemental silver would be oxidized subsequently by iron (III):

$$Ag(s) + Fe^{3+} \longrightarrow Ag^+ + Fe^{2+} \tag{5}$$

Subsequent research in this area examined the interaction of deoxygenated solutions of aqueous silver ions and sulfuric acid with pyrite surfaces in the absence of iron (III) sulfate [5, 6], using various techniques such as XPS, SEM and voltammetry. It was determined that silver sulfide and elemental silver were formed on the pyrite surface. This interaction was examined in terms of possible cathodic and anodic reactions [5, 6], as follows:

Anodic reactions:

$$FeS_2(s) + 8H_2O \longrightarrow Fe^{2+}(aq) + 2SO_4^{2-}(aq) + 16H^+ + 14e^- \tag{6}$$

$$FeS_2(s) \longrightarrow Fe^{2+}(aq) + 2S(s) + 2e^- \tag{7}$$

Cathodic reaction

$$2Ag^+(aq) + S(s) + 2e^- \longrightarrow Ag_2S(s) \tag{8}$$

Overall reaction:

$$4FeS_2(s) + 14Ag^+(aq) + 4H_2O \longrightarrow 4Fe^{2+}(aq) + 7Ag_2S(s) + SO_4^{2-}(aq) + 8H^+ \tag{9}$$

0021-891X

The probable process for the formation of metallic silver is a simple one-electron reduction of silver ion:

$$Ag^+(aq) + e^- \longrightarrow Ag(s) \qquad (10)$$

Other surface studies have been performed under different conditions, such as different pH and silver ion concentration, and have found silver sulfide, metallic silver and polysulfides on the pyrite surface [7, 8].

Raman studies have shown that anodic oxidation of pyrite initially produces polysulfides, but as oxidation proceeds, elemental sulfur becomes the predominant feature [9]. Electrochemical studies in 0.25 mol dm^{-3} sulfuric acid indicate the presence of sulfur through the presence of two peaks at −95 mV vs SCE (cathodic peak) and −80 mV vs SCE (anodic peak) which have been assigned to the reduction and oxidation of sulfide ion [6]:

$$S + 2H^+ + 2e^- \longrightarrow H_2S \qquad (11)$$

It has also been suggested that the sulfur is actually present as a metal-deficient sulfide.

Recent work [10] has led to the conclusion that the open circuit potential (or rest potential) of pyrite is a corrosion potential. It is believed that under acidic conditions, the following reactions contribute to this potential [10–12]:

Anodic reaction:

$$2xh^+ + FeS_2(s) \longrightarrow Fe_{1-x}S_2(s) + xFe^{2+}(aq) \qquad (12)$$

$$xFe^{2+}(aq) + 2xH_2O + xh^+ \longrightarrow xFeOOH(s) + 3xH^+ \qquad (13)$$

Cathodic reaction:

$$FeS_2(s) + 2xH^+ + 2xe^- \longrightarrow FeS_{2-x}(s) + xH_2S(aq) \qquad (14)$$

where h^+ represents holes arising from surface states in pyrite. At the open-circuit potential, or at more negative potentials where silver ion might be expected to be reduced, elemental sulfur is absent.

From the above discussion it can be seen that the mechanism of formation of silver sulfide and elemental silver on pyrite surfaces is not clearly understood. The reason for this is that until recently there was ambiguity concerning the mechanism for dissolution of pyrite and the nature of the major products.

The purpose of this research is to investigate the interaction of silver ions with pyrite at pH 3 in aqueous solutions at room temperature using cyclic voltammetry and a pyrite rotating disc electrode (RDE), in order to provide a better understanding of the mechanism for deposition of silver on pyrite.

2. Experimental details

2.1. *Materials*

Pyrite crystals were obtained from Wards Natural Science Establishment Inc. and originated from either Soria or Logrono, Spain. To construct the rotating disc electrode, pyrite cylinders were cut with a diamond core drill perpendicular to the (1 0 0) crystal face. Only samples free from visible inclusions were used. All pyrite samples were n-type semiconductors [13].

2.2. *Electrochemical measurements*

Electrochemical measurements were obtained with an EG&G Princeton Applied Research model 273 potentiostat/galvanostat controlled by a computer. Positive currents are oxidative. Rotating disc experiments were performed with Pine Instruments Co. models ASR2 rotator and ACMDI2805 arbor. A three-electrode electrochemical cell was used for all measurements. All potentials (unless specified otherwise) are reported relative to the saturated calomel electrode (SCE). The working electrode compartment was separated from the reference and counter electrode compartments with glass frits. The compartment containing the SCE contained only supporting electrolyte, with no silver ions. A few experiments were done using an etched silver wire as the reference electrode, the tip of which was placed about 5 mm from the edge of the electrode. The overpotential at which silver deposition commenced (see below) was the same within 2 mV, indicating absence of effects from *iR* drop or liquid junction potentials.

All electrolytes were prepared with doubly-distilled water. Solutions were made with BDH analytical reagent grade sodium nitrate ($NaNO_3$) and nitric acid (HNO_3) or sodium sulfate (Na_2SO_4) and sulfuric acid (H_2SO_4). For all experiments the electrolytes were deaerated with nitrogen gas from which trace amounts of oxygen were removed from the nitrogen gas by passing through a 30 cm column of BASF R3-11 catalyst. The electrochemical cell was immersed in a water bath at room temperature 25 ± 1 °C.

The rotating disc electrode (RDE) was wet polished prior to each experiment with 800 and 1200 grit silicon carbide followed by 10 μm borocarbide and $\frac{1}{2}$ μm diamond wet laps. After rinsing, the electrode was immediately placed in the cell.

pH measurements were recorded with an Orion SA 720 pH meter and a Radiometer 6K 733526 combination electrode. Kinematic viscosities were measured at 25.0 °C using a Cannon–Ubbelohde capillary viscometer with a flow time for water of 334 s.

3. Results and discussion

Figure 1 shows a cyclic voltammogram for a pyrite electrode immersed in a solution of 1 mmol dm^{-3} silver nitrate, plus 1 mol dm^{-3} sodium nitrate, adjusted to pH 3 with nitric acid.

The cell potential for peak I (estimated as the potential at which the current just departs from zero) occurs at approximately 326 mV vs SCE and is observed only at a silver nitrate concentration of 1 mmol dm^{-3} (Fig. 1). The Nernst equation was used to calculate the cell potential for silver deposition at 25 °C, assuming that

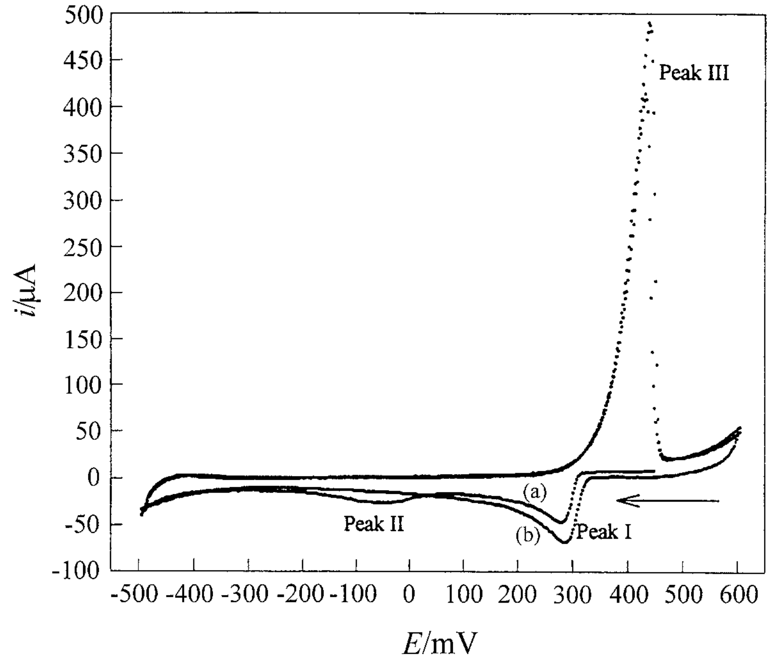

Fig. 1. Cyclic voltammogram for a stationary pyrite electrode immersed for 15 min in 1 mmol dm^{-3} $AgNO_3$ + 1 mol dm^{-3} $NaNO_3$, pH 3, sweep rate 20 mV s^{-1}. (a) First scan: initial potential (open-circuit) 450 mV, limits −495 to +605 mV; (b) second scan, limits +605, −495 mV.

the activity of the silver metal substrate is unity (i.e. the surface is covered with metallic silver):

$$E/\mathrm{V(SCE)} = 0.554 + 0.0257 \ln([\mathrm{Ag}^+] y_{\mathrm{Ag}^+}/c^\circ) \quad (15)$$

where $c^\circ = 1$ mol dm^{-3} is the standard concentration, and y is the activity coefficient for silver ion in a 1 mol dm^{-3} solution of sodium nitrate. The activity coefficient for silver ion was estimated using the equations of Pitzer [14] (in molality form), with interaction coefficients $\beta^{(0)}$, $\beta^{(1)}$, C^ϕ for the pairs H^+–NO_3^-, Na^+–NO_3^- and Ag^+–NO_3^- obtained from tables in [14]. Densities calculated from [15] were used to first convert concentrations to molalities, and finally to convert the activity coefficient from the molality to the concentration scale. The value found was $y_{\mathrm{Ag}^+} = 0.386$.

From the calculated cell potential for reduction of silver ions, 352 mV vs SCE, peak I has been assigned to the electrochemical deposition of metallic silver, Equation 10. The observed cell potential, 326 mV vs SCE, is lower than the calculated value by 26 mV. The difference can be ascribed either (i) to a concentration of silver ions at the pyrite surface which is lower than the bulk concentration, or (ii) nucleation and growth of the deposit, so that the activity of metallic silver is less than unity in the initial stages of deposition. Case (i) can arise because, at the open circuit potential, silver ions are being consumed by chemical reaction with the pyrite surface to form silver sulfide, Ag_2S:

$$2\mathrm{Ag}^+(\mathrm{aq}) + \mathrm{H_2S(aq)} \longrightarrow \mathrm{Ag_2S(s)} + 2\mathrm{H}^+ \quad (16)$$

Peak I is not observed at lower silver concentrations because at the electrode surface all the free Ag^+ has been consumed by the chemical reaction (Equation 16).

Other experiments, carried out at a rotating electrode in a solution of 1 mmol dm^{-3} silver nitrate, 1 mol dm^{-3} sodium nitrate maintained at pH 3 with nitric acid, examined the effect of rotation. Limiting currents were reached at a potential of about +165 mV vs SCE. The limiting current for peak I is linear in the square root of the angular speed of rotation (ω), which confirms a diffusion-limited reaction. From the Levich equation, the diffusion coefficient for the silver ion can be estimated [16]:

$$i_{\mathrm{L}} = 0.62 nFAD^{2/3} \nu^{-1/6} c^\infty \omega^{1/2} \quad (17)$$

Here, i_{L} is the limiting current, ω is the angular speed, $n(= 1)$ is the number of electrons involved in the reaction, F is the Faraday constant (96486.7 C mol^{-1}), c^∞ is the bulk concentration of silver nitrate (10^{-3} mol dm^{-3}), A is the surface area of the pyrite electrode (0.292 cm^2) and ν is the measured kinematic viscosity ($(8.96 \pm 0.18) \times 10^{-3}$ cm^2 s^{-1}). Using the Levich equation and the slope from limiting current against the square root of the angular velocity, for peak I, the diffusion coefficient for silver ions was estimated to be $(1.57 \pm 0.13) \times 10^{-5}$ cm^2 s^{-1} compared to the value at infinite dilution of 1.647×10^{-5} cm^2 s^{-1} calculated from

$$D^\infty(\mathrm{Ag}^+) = RT\lambda^\infty/F^2 \quad (18)$$

where R is the gas constant, $T(= 289\ \mathrm{K})$ is the thermodynamic temperature and $\lambda^\infty(= 6.19 \times 10^{-3}$ S m^2 mol^{-1}) is the molar ionic conductivity at infinite dilution of silver ion [17]. This provides further evidence that peak I is due to the deposition of metallic silver. It was also noted that the cell potential for peak I became more positive with increasing angular speed, reaching 340 mV vs SCE at 500 rpm.

The peak current for peak I is linear in the square root of the sweep rate. For sweep experiments producing metal deposition, Berzins and Delahay [18] showed that the peak current density is

$$I_p = -0.5410\,nFc^{\infty}D^{1/2}\left(\frac{nF}{RT}\right)^{1/2}\gamma^{1/2} \qquad (19)$$

where γ is the sweep rate. From previous rotation experiments the diffusion coefficient was found to be $1.57 \times 10^{-5}\,\mathrm{cm^2\,s^{-1}}$, therefore the slope of peak current against the square root of the sweep rate should be $-1.29 \times 10^{-3}\,\mathrm{A\,cm^2\,V^{-1/2}\,s^{1/2}}$. The measured slope is $-1.12 \times 10^{-3}\,\mathrm{A\,cm^{-2}\,V^{-1/2}\,s^{1/2}}$, confirming that the reaction is diffusion controlled with respect to silver ions. The peak potential is

$$E_p = E^{\circ} + \frac{RT}{nF}\ln yc^{\infty} - 0.8540\frac{RT}{nF} \qquad (20)$$

which is independent of sweep rate. Berzins and Delahay [18] assumed that the activity of the deposited metal was unity, that is, the surface was covered initially with silver. Krebs and Roe [19] derived a numerical solution for the case of metal deposition with nucleation and hemispherical growth of the deposit. The same dependence of current on sweep rate was found. Although the dependence of peak potential on sweep rate was not discussed, it appears to depend somewhat on the amount of metal deposited initially. The peak potential for peak I is independent of sweep rate at low sweep rate, but does show some variation at higher sweep rates (Fig. 2). If there is a surface ion exchange reaction which consumes silver ions and is rapid compared to the rate of diffusion, the surface sites will become saturated with silver ions very quickly. The surface concentration of silver ion in solution will drop until all available surface sites have become occupied by silver ions, and then relax by diffusion towards the bulk value as time increases. The total charge passed and the time of electrolysis both decrease with increasing sweep rate over roughly the same potential range. The result is that, at longer times of electrolysis the effect of the initial gradient arising from the ion-exchange reaction is less, giving a more positive cell potential, as observed.

Berzins and Delahay [18] observed changes in peak potential with scan rate for the deposition of cadmium, but the peak potential shifted in a negative direction rather than in a positive direction as observed here.

Figure 3 shows the relation between immersion time (time that the electrode is immersed in solution before scan is started) and peak current for Peak I which supports the interpretation of Fig. 2. The peak current, i_p, is proportional to c^{∞} which has been assumed to be the bulk silver ion concentration, but the theory shows that this is actually the initial surface concentration of silver ions. The times to reach the peak current are a few seconds at most, while the immersion time required to reach a constant peak current is about 10 min. Therefore, the peak current of the voltammetric scan serves as a probe of the silver ion concentration at the surface. With increasing immersion time the peak current reaches a limiting value, which is consistent with the consumption of silver ions in a chemical reaction with the pyrite surface. The peak current is lower at shorter times because silver ions have been removed from the diffusion layer through chemical reaction with the pyrite surface. At longer times, the peak current is higher because the surface sites have become covered with silver ions and the surface concentration in solution is relaxing by diffusion to its bulk value.

Figures 4 and 5 show cyclic voltammograms for a

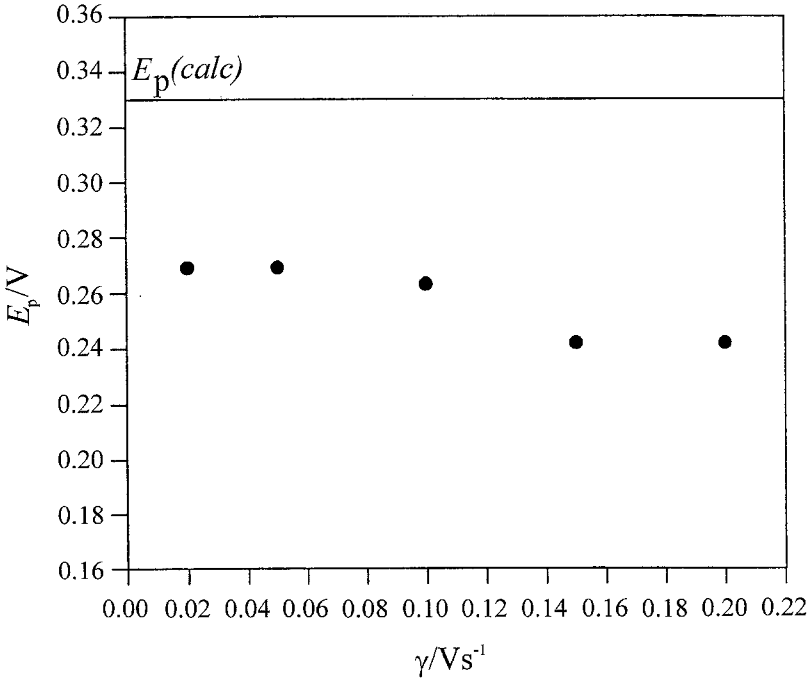

Fig. 2. Peak potential, E_p, as a function of sweep rate, γ, for peak I. (——) represents the theoretical peak potential calculated from Equation 20.

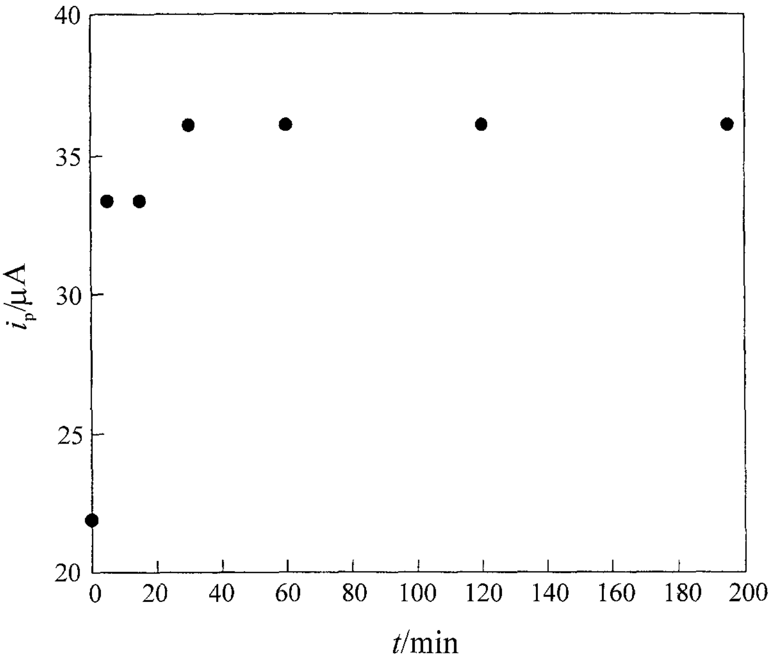

Fig. 3. Peak current, i_p, as a function of immersion time, t, for peak I; sweep rate 20 mV s^{-1}.

pyrite electrode immersed in solutions of 0.1 and 0.01 mmol dm^{-3} silver nitrate, plus 1 mol dm^{-3} sodium nitrate, and adjusted to pH 3 with nitric acid. The cell potential for peak II varies between 29.4 mV vs SCE at $[Ag^+] = 1$ mmol dm^{-3} and 128 mV vs SCE at $[Ag^+] = 0.01$ mmol dm^{-3} (Table 1). There is no observable corresponding anodic peak, which suggests irreversible behaviour. Peak II is not observed when there is no silver ion present, and only on the first scan even in the presence of silver ion (Fig. 1). The peak current rises quickly and reaches a relatively constant value, 25 ± 3 μA, with immersion time. It is unlikely that peak II is due to pyritic sulfur reduction: based on studies done in 1 mol dm^{-3} sodium nitrate at pH 3, the sulfur reduction peak is observed at −300 mV vs SCE. These observations are consistent with a surface species being formed chemically at the open circuit potential, and consequently being reduced during the cyclic voltammogram. We propose that this surface species is formed by replacement of Fe^{2+} with Ag^+:

$$2yAg^+(aq) + Fe_{1-x}S_2(s) \longrightarrow Fe_{1-x-y}Ag_{2y}S_2(s) + yFe^{2+}(aq) \qquad (21)$$

where some initial loss of Fe^{2+} by dissolution of pyrite is assumed. Other analogous ion exchange mechanisms have been proposed for two Ag^+ exchanging

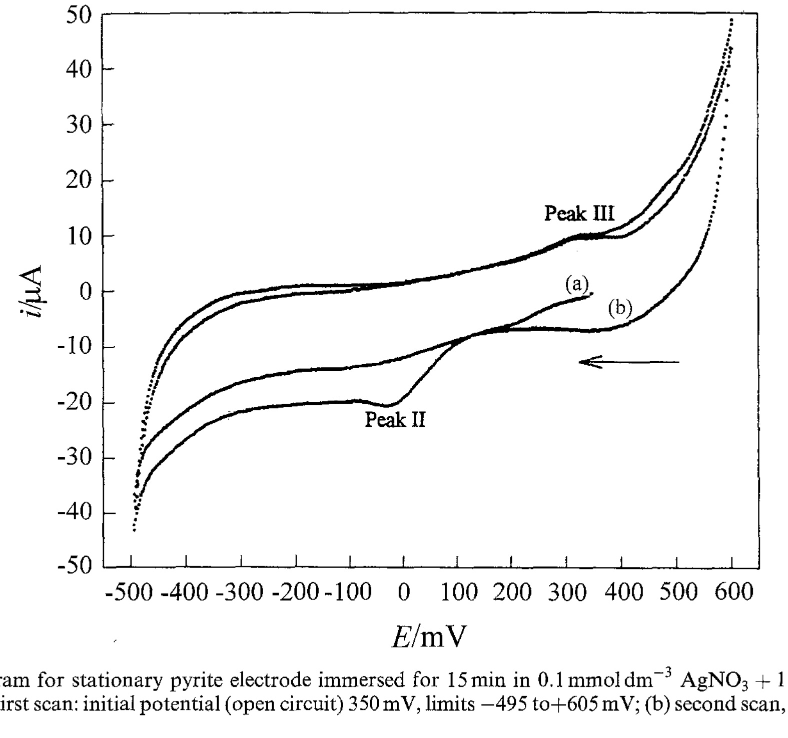

Fig. 4. Cyclic voltammogram for stationary pyrite electrode immersed for 15 min in 0.1 mmol dm^{-3} $AgNO_3$ + 1 mol dm^{-3} $NaNO_3$, pH 3, sweep rate 20 mV s^{-1}. (a) First scan: initial potential (open circuit) 350 mV, limits −495 to +605 mV; (b) second scan, limits +605 to −495 mV.

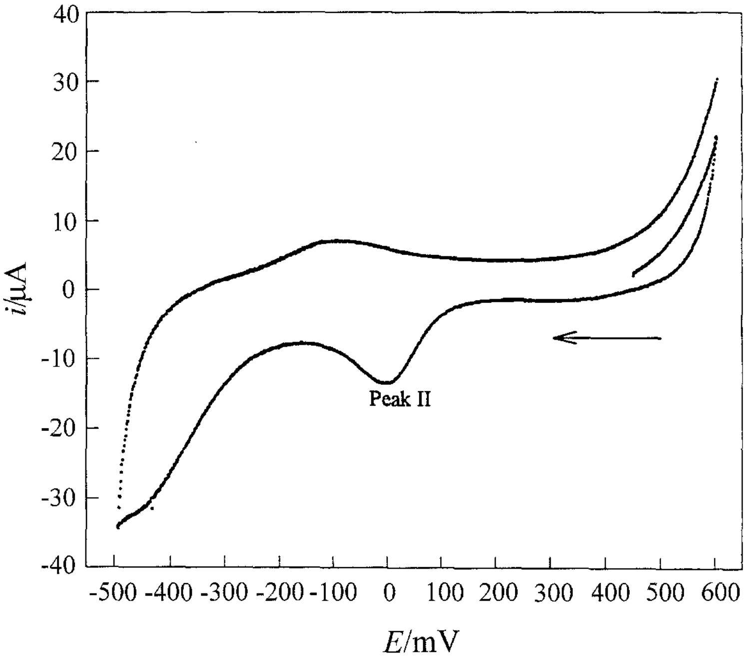

Fig. 5. Cyclic voltammogram for stationary pyrite electrode immersed for 15 min in 0.01 mmol dm^{-3} AgNO$_3$ + 1 mol dm^{-3}, NaNO$_3$, pH 3, sweep rate 20 mV s^{-1}. Scan: +450 to +605 to −500 to +605 mV.

for Pb^{2+} in galena [8]. Peak II is then assigned to the reduction of $Fe_{1-x-y}Ag_{2y}S_2$, in which some of the excess surface sulfur is removed:

$$Fe_{1-x-y}Ag_{2y}S_2(s) + 2zH^+ + 2ze^- \longrightarrow Fe_{1-x-y}Ag_{2y}S_{2-z}(s) + zH_2S(aq) \qquad (22)$$

This reaction cannot be established unequivocally from these experiments.

Peak III (Figs 1 and 4) is found between 255 mV vs SCE at $[Ag^+] = 0.1$ mmol dm^{-3} and 285 mV vs SCE at $[Ag^+] = 1$ mmol dm^{-3} (Table 2). Again the dissolution of metallic silver starts at a much lower potential than expected, probably because there is a small concentration of silver ions in equilibrium with silver metal in the diffusion layer. It is noted that there is no peak III associated with a silver concentration of 0.01 mmol dm^{-3}, probably because silver ions are consumed in the formation of silver sulfide and metallic silver is not formed at the open circuit potential. From the above discussion peak III has been assigned to the dissolution of metallic silver (reverse of Equation 10).

Table 1. Effect of silver ion concentration on the cell potential for peak II

[Ag$^+$] /mmol dm^{-3}	*E (obs)* /mV
1	29.4
0.1	100
0.01	128

Table 2. Calculated and observed cell potentials for the dissolution of metallic silver (peak III). Also shows the concentrations of silver ion corresponding to the observed cell potentials

{Ag$^+$} /mmol dm^{-3}	*E (calc)* /mV	*E (obs)* /mV	*[Ag$^+$] (calc)* /mmol dm^{-3}
1	352	285	0.074
0.1	293	255	0.023
0.01	234	(not obsd.)	–

Figure 6 shows a similar dependence of peak current on immersion time as in Fig. 3. The current increases at short times and approaches a limiting value with increasing time, again suggesting that initially some of the silver ions are consumed in a chemical reaction at the pyrite surface.

Further evidence for the assignment of peaks II and III is provided with a number of voltammograms run under different conditions. Figure 7 shows a cyclic voltammogram for a pyrite electrode in a solution containing no silver ions. The poor quality of the plot is due to instrumental limitations at the low currents encountered. The electrode had been immersed for 2 h in a solution of 1 mmol dm^{-3} silver nitrate and 1 mmol dm^{-3} sodium nitrate adjusted to pH 3 with nitric acid before the voltammogram was run. Peak I is not observed, which is expected as there are no free silver ions to deposit on the surface, but peaks II and III are present. The presence of peak II suggests that $Fe_{1-x-y}Ag_{2y}S_2$ is formed at open circuit potentials. The presence of peak III suggests that silver metal has been deposited on the pyrite surface probably through reduction of the $Fe_{1-x-y}Ag_{2y}S_{2-z}$ at a potential around −420 mV vs SCE. Another peak IV is observed at about −350 mV vs SCE, which from previous studies [6] can be assigned to the oxidation of metallic silver in the presence of sulfide (formed through reactions occurring at the open circuit potential, and also produced at peak II) to produce silver sulfide:

$$2Ag(s) + H_2S(aq) \longrightarrow Ag_2S(s) + 2H^+ + 2e^- \qquad (23)$$

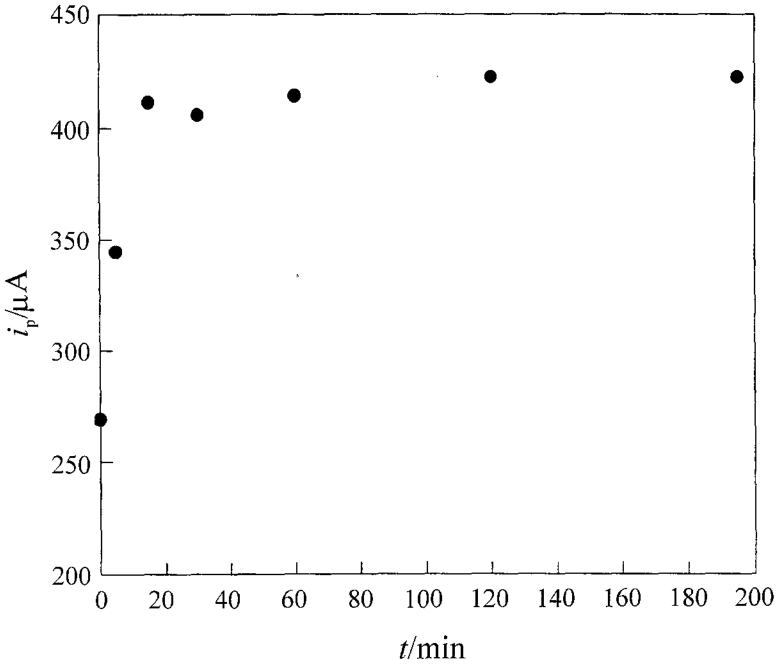

Fig. 6. Peak current i_p, as a function of immersion time, t, for peak III.

Figure 8 shows a cyclic voltammogram for a pyrite electrode immersed in a solution of 1 mmol dm^{-3} silver nitrate and 0.25 mol dm^{-3} sulfuric acid. Peak I is again assigned to the deposition of metallic silver (Reaction 10). Peak V occurs at −390 mV vs SCE and has previously [6] been assigned to the reduction of silver sulfide:

$$Ag_2S(s) + 2H^+ + 2e^- \longrightarrow 2Ag(s) + H_2S(aq) \qquad (24)$$

Peak IV at −260 mV vs SCE has previously [6] been assigned to metallic silver oxidation to form silver sulfide, Reaction 23, while peak III is due to silver dissolution.

Figure 9 shows a cyclic voltammogram for a pyrite electrode immersed in a solution of 1 mmol dm^{-3} Ag^+ and 0.25 mol dm^{-3} H_2SO_4 for 2 h, and then run in a fresh solution with no silver ions present. As expected, the same peaks as in Fig. 8 are present except for peak I, which is absent because there were no free silver ions to be reduced. These experiments suggest the formation of a layer of silver sulfide on the pyrite surface, based on what has been reported [5–8] previously.

The experiments producing Figs 7, 8 and 9 add

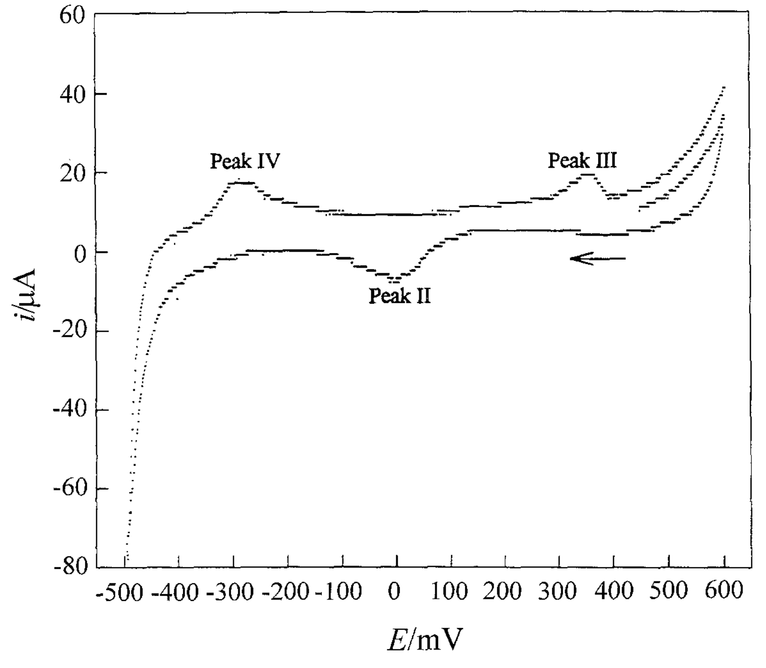

Fig. 7. Cyclic voltammogram for stationary pyrite electrode immersed in 1 mmol dm^{-3} $AgNO_3$ + 1 mol dm^{-3} $NaNO_3$, pH 3, for 2 h, then run in fresh solution with no Ag^+; sweep rate 20 mV s^{-1}, scan +450 to +605 to −495 to +605 mV.

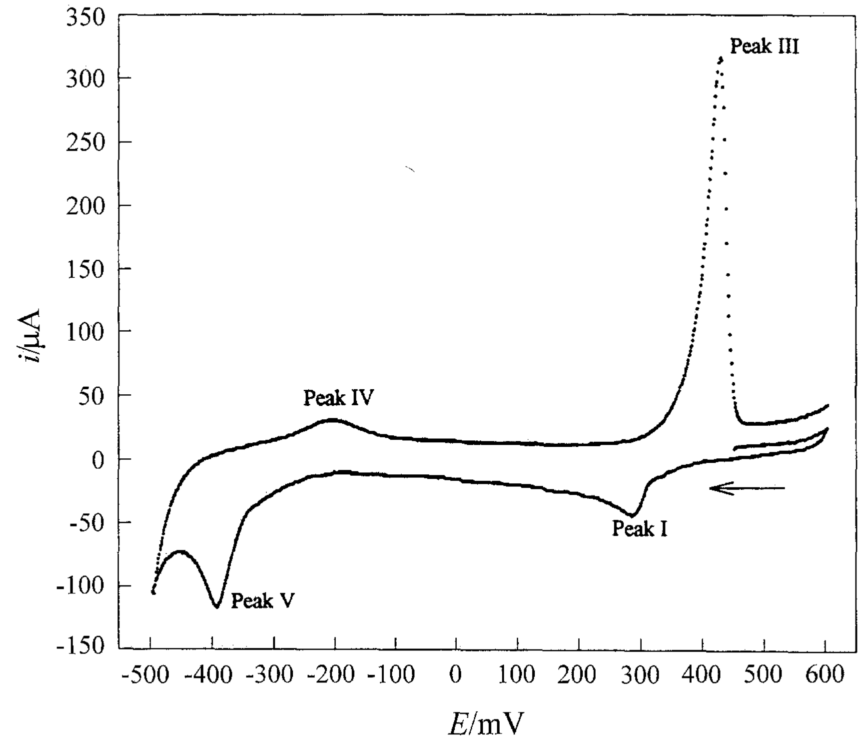

Fig. 8. Cyclic voltammogram for stationary pyrite electrode immersed in 1 mmol dm^{-3} $AgNO_3$ and 0.25 mol dm^{-3} H_2SO_4 for 15 min, sweep rate 20 mV s^{-1}. Scan: +450 to +605 to −495 to +605 mV.

support to the idea of a 'AgS' complex different from Ag_2S. These results suggest that peak II is indeed not Ag_2S, as the reduction potential is not in the expected potential range as suggested in Figs 8 and 9. However, Fig. 7 does seem to show the same anodic peaks as observed in Fig. 9, suggesting that peak II is related to some form of 'AgS' which is reduced at very negative potential to produce similar reduction products as that for Ag_2S, as they can be seen to be oxidized on the positive scan. This information lends credence to the idea of a surface iron–silver sulfide species, $Fe_{1-x-y}Ag_{2y}S_2$.

4. Conclusion

The above experiments show that the interaction of silver ion with pyrite involves the products formed from the dissolution of pyrite. Silver ions reacts very rapidly with an iron-deficient sulfide to form an

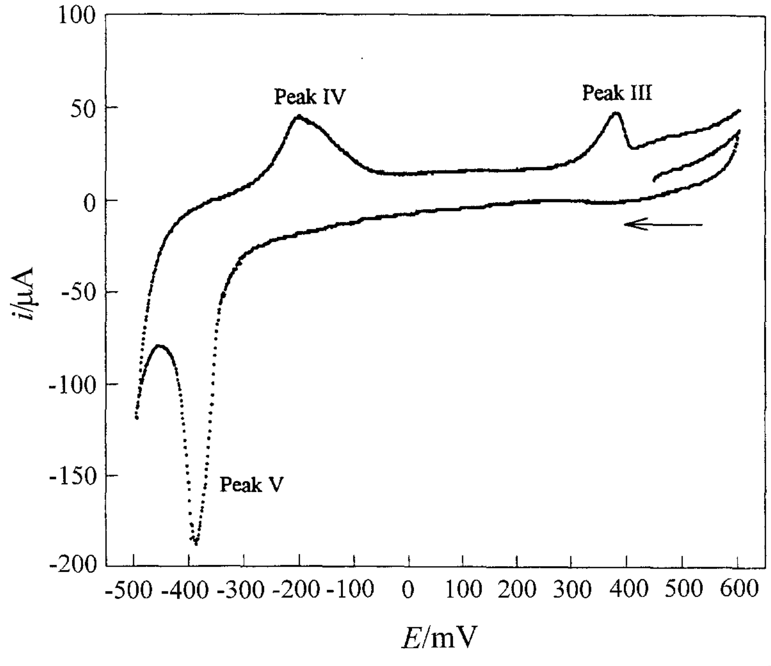

Fig. 9. Cyclic voltammogram for stationary pyrite electrode immersed in 1 mmol dm^{-3} $AgNO_3$ and 0.25 mol dm^{-3} H_2SO_4 for 2 h, then run in fresh solution with no Ag^+, sweep rate 20 mV s^{-1}. Scan: +450 to +605 to −495 to +605 mV.

iron–silver sulfide surface species, leading to a decreased silver ion concentration at the surface. The interaction with iron (II) ions appears to be a simple ion exchange reaction similar to that which has been demonstrated recently [8] for the interaction of silver ions with galena.

REFERENCES

[1] J. D. Miller and H. Q. Portillo, *in* 'Mineral Processing' (edited by J. Laskowski), Elsevier, Amsterdam (1981) pp. 851–901.

[2] D. W. Price and G. W. Warren, *Hydrometallurgy* **15** (1986) 325.

[3] A. J. Parker, R. L. Paul and G. P. Power, *J. Electroanal. Chem.* **118** (1981) 305.

[4] J. B. Hiskey, P. P. Phule and M. D. Pritzker, *Metall. Trans. B* **18** (1987) 641.

[5] J. B. Hiskey and M. D. Pritzker, *J. Appl. Electrochem.* **18** (1988) 484.

[6] A. N. Buckley, H. J. Wouterlood and R. Woods, *J. Appl. Electrochem.* **19** (1989) 744.

[7] G. M. Bancroft and M. M. Hyland, *in* 'Mineral-Water Interface Geochemistry' (edited by P. H. Ribbe), Mineralogical Society of America, **23** (1990) pp. 511–58.

[8] M. J. Scaini, G. M. Bancroft, J. W. Lorimer and L. M. Maddox, *Geochim. Cosmochim. Acta* **59** (1995) 2733.

[9] J. R. Mycroft, G. M. Bancroft, N. S. McIntyre, J. W. Lorimer and I. R. Hill, *J. Electroanal. Chem.* **292** (1990) 139.

[10] J. R. Mycroft, G. M. Bancroft and J. W. Lorimer, *J. Electroanal. Chem.* submitted.

[11] K. Osseo-Asare, *Hydrometallurgy* **29** (1992) 61.

[12] K. K. Mishra and K. Osseo-Asare, *J. Electrochem. Soc.* **135** (1988) 2502.

[13] J. R. Mycroft, 'Electroless Reduction of Gold (III) on Pyrite from Chloride Electrolytes', PhD thesis, The University of Western Ontario, London, Canada, (1993).

[14] K. S. Pitzer, *in* 'Activity Coefficients in Electrolyte Solutions', vol. 1 (edited by R. M. Pytkowicz), CRC Press, (1979), chapter 7.

[15] I. D. Zaytsev and G. G. Aseyev (eds), 'Properties of Aqueous Solutions of Electrolytes' (translated by M. A. Laxarev and V. R. Sorochenko) CRC Press, (1992).

[16] Southampton Electrochemistry Group, 'Instrumental Methods in Electrochemistry', Ellis Horwood (1985).

[17] R. A. Robinson and R. H. Stokes, 'Electrolyte Solution', Butterworth, 2nd edn, (1959).

[18] T. Berzins and P. Delahay, *J. Amer. Chem. Soc.* **75** (1953) 555.

[19] W. M. Krebs and D. K. Roe, *J. Electrochem. Soc.* **114** (1967) 892.